

# Calculation of the Mass Spectrum of QED-2 in Light-Front Coordinates

S. A. Paston\*, E. V. Prokhvatilov† V. A. Franke‡  
*St.-Petersburg State University, Russia*

## Abstract

With the aim of a further investigation of the nonperturbative Hamiltonian approach in gauge field theories, the mass spectrum of QED-2 is calculated numerically by using the corrected Hamiltonian that was constructed previously for this theory on the light front. The calculations are performed for a wide range of the ratio of the fermion mass to the fermion charge at all values of the parameter  $\hat{\theta}$  related to the vacuum angle  $\theta$ . The results obtained in this way are compared with the results of known numerical calculations on a lattice in Lorentz coordinates. A method is proposed for extrapolating the values obtained within the infrared-regularized theory to the limit where the regularization is removed. The resulting spectrum agrees well with the known results in the case of  $\theta = 0$ ; in the case of  $\theta = \pi$ , there is agreement at small values of the fermion mass (below the phase-transition point).

---

\*E-mail: paston@pobox.spbu.ru

†E-mail: Evgeni.Prokhvat@pobox.spbu.ru

‡E-mail: franke@pobox.spbu.ru

## 1. Introduction

The Hamiltonian approach to quantum-field theory in light-front coordinates  $x^\pm = (x^0 \pm x^3)/\sqrt{2}$ ,  $x^\perp = (x^1, x^2)$ , where  $x^+$  plays the role of time [1], is one of the nonperturbative methods for solving the problem of strong interaction [2, 3]. Within this approach, the quantization is performed in the  $x^+ = 0$  plane, the generator  $P_+$  of a shift along the  $x^+$  axis playing the role of the Hamiltonian. The generator  $P_-$  of a shift along the  $x^-$  axis does not displace the quantization surface; therefore, it is a kinematical generator (according to Dirac's terminology) in contrast to the dynamical generator  $P_+$ . As a result, the momentum operator  $P_-$  appears to be quadratic in fields and does not depend on interaction. At the same time, the operator  $P_-$  is nonnegative and has zero eigenvalue only on the physical vacuum. This results in that the field Fourier modes corresponding to positive and negative values of  $p_-$  play the role of, respectively, creation and annihilation operators over the physical vacuum and can be used to construct Fock space. Thus, we see that, in light-front coordinates, the physical vacuum formally coincides with the mathematical vacuum.

The spectrum of bound states in the theory can be sought by solving the Schroedinger equation

$$P_+|\Psi\rangle = p_+|\Psi\rangle \quad (1)$$

in the subspace specified by fixed  $p_-$  and  $p_\perp$  and by employing the expression  $m^2 = 2p_+p_- - p_\perp^2$  for the mass. This search for bound states can be performed beyond perturbation theory – for example, with the aid of so-called method of discrete light-cone quantization [2, 4].

However, the light-front Hamiltonian formalism involves a specific divergence at  $p_- = 0$  [2, 3], and it must be regularized. The introduction of a cutoff  $|p_-| \geq \varepsilon > 0$ , which violates Lorentz and gauge invariance, is one of the methods for its regularization. A cutoff  $|x^-| \leq L$  that involves imposing (anti)periodic boundary conditions in  $x^-$  (discrete light-cone quantization method, which respects gauge invariance) is yet another possible regularization. In this case, the lightlike momentum  $p_-$  becomes discrete ( $p_- = p_n = \pi n/L$ , where  $n$  is an integer), the field zero mode corresponding to  $n = 0$  being separated explicitly. In principle, the canonical formalism makes it possible to express this zero mode in terms of other modes by solving the constraint equation, but this is difficult as a rule [5, 6].

The regularization of the above divergence usually renders a theory in light-front coordinates nonequivalent to its conventional formulation in Lorentz coordinates [7–9]. This can be revealed even in the lowest orders of perturbation theory [10]. As a result, there arises the problem of correcting the canonical light-front Hamiltonian (which is the result of a "naive" canonical quantization in light-front coordinates) – that is, the problem of seeking counterterms to it that compensate for the above distinctions between the Hamiltonians. If this problem can be solved for a specific theory in all orders of perturbation theory, the resulting corrected light-front Hamiltonian can then be used to perform nonperturbative calculations.

The aforementioned formal coincidence of the physical and the mathematical vacuum becomes rigorous only after the introduction of regularization, upon which the vicinity of the point  $p_- = 0$  is eliminated – for example, after the introduction of the cutoff  $|p_-| \geq \varepsilon > 0$ . If the corrected light-front Hamiltonian can be constructed for a theory regularized in this way, then vacuum effects inherent in the original theory in Lorentz coordinates must be taken into account with the aid of additional terms of this Hamiltonian.

The problem of constructing the corrected canonical light-front Hamiltonian was successfully solved both for nongauge field theories of the Yukawa model type [11] and for QCD in the gauge  $A_- = 0$  [12]. In the last case, however, the corrected light-front Hamiltonian was constructed only for specific ultraviolet and infrared regularizations violating gauge invariance. As a result, it appears that the corrected Hamiltonian involves a large number of indeterminate coefficients; only for some, a priori unknown, dependence of these coefficients on the regularization parameter does it reproduce, in the limit where the regularization is removed, the results of the Lorentz-covariant theory in all orders of perturbation theory. The practical calculations with the resulting Hamiltonian are very cumbersome because of the presence of unknown coefficients and because of a complicated structure of regularization (the regularized Hamiltonian involves a large number of additional fields).

In view of these circumstances, it is desirable to seek alternative methods for constructing the correct light-front Hamiltonian for gauge theories. In this connection, it is of interest to study the simplest models that admit a nonperturbative approach – in particular, those where one can study the behavior of infinite series of perturbation theory in all orders. Two-dimensional QED (QED-2) featuring a nonzero fermion mass (it is also known as the massive Schwinger model) is one of such models. In recent years, this two-dimensional model has attracted attention as an object of application of new methods for studying QCD, since it possesses many properties similar to those of QCD: confinement, chiral-symmetry breaking, and a topological  $\theta$  vacuum (see [13] and references therein, as well as [14–16]). Information obtained in analyzing QED-2 can also be used in developing new methods that take into account nonperturbative vacuum effects and which are appropriate for constructing the light-front Hamiltonian for four-dimensional gauge theories. It should be noted that attempts at extracting information about four-dimensional gauge theories on the light front from an analysis of QED-2 were undertaken earlier [17].

For QED-2, there exists the possibility of going over to an equivalent scalar theory [18] (belonging to the type of the sine-Gordon model). This can be done by means of the bosonization procedure – that is, by going over from the fermion variables to boson ones [9, 19]. Upon this transition, the mass term of the fermion field in the QED-2 Hamiltonian becomes the interaction term for a scalar field, while the fermion mass  $M$  becomes the interaction constant in the boson theory. In the boson theory, the fact that the quantum vacuum in QED-2 has a nontrivial character associated with instantons ( $\theta$  vacuum) [18, 15] is taken explicitly into account with the aid of the parameter  $\theta$  in the interaction term. At  $M = 0$ , QED-2 reduces to the Schwinger model, while the equivalent boson theory appears to be free.

Perturbation theory for a boson theory (perturbation theory in the fermion mass) is usually referred to as chiral perturbation theory. For this kind of perturbation theory, ultraviolet finiteness was proven in [20, 21]. By analyzing perturbation theory in all orders of  $M$ , one can construct a corrected light-front Hamiltonian in terms of bosons and, after this, return to the fermion variables [21, 22]. It should be noted that boson perturbation theory differs radically from perturbation theory in the coupling constant of the original theory involving fermions (in QED-2, the latter perturbation theory does not exist at all because of infrared divergences, and this was the reason for introducing bosonization). Therefore, the resulting light-front Hamiltonian can take into account nonperturbative (in the conventional coupling constant) effects. But at the same time, it can fail to describe effects that are nonperturbative in the fermion mass – for example, phase transitions.

It is well known that, at least at the vacuum-angle value of  $\theta = \pi$ , there is a phase transition in QED-2 at some value of the fermion mass  $M$  (see, for example, [13]). It should be expected that, in the presence of a phase transition, which is accompanied by the appearance of nonzero vacuum expectation values of some operators, the correct light-front Hamiltonian must have different form for different phases, since the light-front vacuum itself is always trivial. Therefore, the results of calculations performed with a specific Hamiltonian must be valid only within one phase. The calculations performed in the present study corroborate these considerations and make it possible to determine the presence and an approximated position of the phase-transition point. A similar phenomenon was discovered previously in the simple two-dimensional  $\lambda\varphi^4$  scalar-field model (see [9, 23], where an approximate method was proposed for going over to the Hamiltonian describing a different phase).

In this study, we perform a numerical nonperturbative calculation of the mass spectrum of the corrected light-front QED-2 Hamiltonian constructed in [21, 22]. The results obtained in this way are compared with the results of numerical calculations on a lattice in Lorentz coordinates from [14, 13].

## 2. Corrected light-front Hamiltonian for QED-2

The QED-2 Lagrangian density in Lorentz coordinates has the form

$$L = -\frac{1}{4}F_{\mu\nu}F^{\mu\nu} + \bar{\Psi}(i\gamma^\mu D_\mu - M)\Psi, \quad (2)$$

where  $F_{\mu\nu} = \partial_\mu A_\nu - \partial_\nu A_\mu$ ,  $D_\mu = \partial_\mu - ieA_\mu$ ,  $A_\mu(x)$  is an Abelian gauge field,  $\Psi$  and  $\bar{\Psi} = \Psi^+\gamma^0$  are two-component fermion fields of mass  $M$ ,  $e$  is the coupling constant, and the matrices  $\gamma^\mu$  are chosen in the form

$$\gamma^0 = \begin{pmatrix} 0 & -i \\ i & 0 \end{pmatrix}, \quad \gamma^1 = \begin{pmatrix} 0 & i \\ i & 0 \end{pmatrix}. \quad (3)$$

In terms of Lorentz coordinates, the Lagrangian density for the boson theory equivalent to QED-2 can be written in the form [21]

$$L = \frac{1}{8\pi} \left( \partial_\mu \varphi \partial^\mu \varphi - m^2 \varphi^2 \right) + \frac{\gamma}{2} e^{i\theta} : e^{i\varphi} : + \frac{\gamma}{2} e^{-i\theta} : e^{-i\varphi} :, \quad \gamma = \frac{Mme^C}{2\pi}, \quad m = \frac{e}{\sqrt{\pi}}, \quad (4)$$

where  $C = 0.577216$  is the Euler constant,  $\theta$  is a quantity that parametrizes the  $\theta$  vacuum of the fermion formulation of the theory, and the normal-ordering symbol means that diagrams with connected lines are excluded in perturbation theory in  $\gamma$  (this corresponds to the usual meaning of the normal-ordering symbol in the Hamiltonian) – it is equivalent to perturbation theory in  $M$ .

In [21, 22], the light-front Hamiltonian generating a theory that describes a one-component fermion field  $\psi$  and which, in the limit where the regularization is removed, is equivalent in all orders in  $\gamma$  to the Lorentz-covariant theory specified by the Lagrangian density (4) was found by using the method described in the Introduction. The theory defined by this Hamiltonian was regularized by the discrete-light-cone-quantization method mentioned in the Introduction:

the cutoff  $|x^-| \leq L$  and the antiperiodic boundary conditions in  $x^-$  were introduced for the field  $\psi$ . The resulting corrected light-front Hamiltonian has the form

$$H = \int_{-L}^L dx^- \left( \frac{e^2}{2} \left( \partial_-^{-1} [\psi^+ \psi] \right)^2 - \frac{eMe^C}{4\pi^{3/2}} \left( e^{-i\hat{\theta}(M/e, \theta)} e^{i\omega} d_0^+ + h.c. \right) - \frac{iM^2}{2} \psi^+ \partial_-^{-1} \psi \right), \quad (5)$$

where  $[...]$  denote the omission of the zero mode in  $x^-$ . The field  $\psi$  is expanded in terms of creation and annihilation operators as

$$\psi(x) = \frac{1}{\sqrt{2L}} \left( \sum_{n \geq 1} b_n e^{-i\frac{\pi}{L}(n-\frac{1}{2})x^-} + \sum_{n \geq 0} d_n^+ e^{i\frac{\pi}{L}(n+\frac{1}{2})x^-} \right), \quad (6)$$

$$\{b_n, b_{n'}^+\} = \{d_n, d_{n'}^+\} = \delta_{nn'}, \quad b_n |0\rangle = d_n |0\rangle = 0. \quad (7)$$

The operator  $\omega$  is the quantity canonically conjugate to the charge operator  $Q$

$$Q = \sum_{n \geq 1} b_n^+ b_n - \sum_{n \geq 0} d_n^+ d_n, \quad (8)$$

which specifies the physical subspace of states,  $|\text{phys}\rangle$ :

$$Q |\text{phys}\rangle = 0. \quad (9)$$

The operator  $\omega$  possesses the properties that completely define it [9, 19],

$$e^{i\omega} |0\rangle = b_1^+ |0\rangle, \quad e^{-i\omega} |0\rangle = d_0^+ |0\rangle \quad (10)$$

and

$$e^{i\omega} \psi(x) e^{-i\omega} = e^{i\frac{\pi}{L}x^-} \psi(x), \quad (11)$$

whence it follows that

$$e^{i\omega} b_n e^{-i\omega} = b_{n+1}, \quad e^{i\omega} d_n^+ e^{-i\omega} = d_{n-1}^+, \quad n \geq 1, \quad e^{i\omega} d_0^+ e^{-i\omega} = b_1. \quad (12)$$

The parameter  $\hat{\theta}$  appearing in the Hamiltonian in (5) is a function of the ratio  $M/e$  and the vacuum angle  $\theta$ . This function is defined as a perturbation-theory series in  $M$ ; therefore, its explicit form remains unknown. Details concerning the appearance of the parameter  $\hat{\theta}$  in the Hamiltonian are considered in the Appendix. Among other things, it is established there that, in the first-order in  $M$ , we have  $\hat{\theta} = \theta$  and that, at any value of  $M$ , the parameter  $\hat{\theta}$  is an odd function of  $\theta$  and takes the value of  $\hat{\theta} = \pi$  at  $\theta = \pi$ . In particular, it follows from the oddness of the function  $\hat{\theta}(\theta)$  that  $\hat{\theta} = 0$  at  $\theta = 0$ . It should be noted that the parameter  $\hat{\theta}$  can be related to the values of the vacuum condensates in the Lorentz-covariant theory [21, 22].

In calculating the mass spectrum of bound states, the quantity  $\hat{\theta}$  is an independent parameter of the theory, along with  $M$  and  $e$ ; the relation between  $\hat{\theta}$  and  $\theta$  for  $\theta \neq 0, \pi$  can in principle be found by comparing the results obtained by calculating the mass spectrum of the theory in Lorentz coordinates and the theory on the light front. We note that expression (5) for the corrected light-front Hamiltonian and the expression obtained upon the naive canonical

quantization of the original fermion theory (2) in the light-front coordinates differ only by the addition of the second term, which is linear in the field operators and which depends on  $\hat{\theta}$  and, hence, on the vacuum angle  $\theta$ . Thus, we see that the naive canonical quantization does not take into account vacuum effects.

The lightlike-momentum operator  $P_-$  has the form

$$P_- = \sum_{n \geq 1} b_n^+ b_n \frac{\pi}{L} \left( n - \frac{1}{2} \right) + \sum_{n \geq 0} d_n^+ d_n \frac{\pi}{L} \left( n + \frac{1}{2} \right). \quad (13)$$

This expression is used to calculate the mass spectrum of bound states.

### 3. Calculation of the mass spectrum of bound states

In order to find the mass spectrum of bound states of the theory, we will seek the eigenvalues  $E_i$  of the fermion light-front Hamiltonian (5) (the subscript  $i$  numbers eigenvalues in the ascending order),

$$H|\Psi_i\rangle = E_i|\Psi_i\rangle \quad (14)$$

in the subspace of physical states at a fixed value of the lightlike momentum (13). This subspace is specified by the conditions

$$Q|\Psi\rangle = 0, \quad P_-|\Psi\rangle = p_-|\Psi\rangle. \quad (15)$$

In view of the antiperiodic boundary conditions and the first of the equalities in (15), the eigenvalue  $p_-$  has the form

$$p_- = \frac{\pi}{L}N, \quad (16)$$

where  $N$  is a nonnegative integer. The bound-state masses  $M_i$  are given by

$$M_i^2 = 2p_-E_i = \frac{2\pi}{L}NE_i. \quad (17)$$

If, in expression (5) for the Hamiltonian, one performs the change of integration variable  $x^- = \frac{L}{\pi}z$  and uses expansion (6), the operator  $\frac{2\pi}{L}NH$ , which determines the quantities  $M_i^2$  does not involve the regularization parameter  $L$  explicitly, but it depends on  $N$ . The quantity  $L$  affects the mass spectrum only through relation (16). Since  $p_-$  does not depend on  $L$ , one can deduce from (16) that the limit  $N \rightarrow \infty$  corresponds to the limit where the regularization is removed,  $L \rightarrow \infty$ .

Since we use the antiperiodic boundary conditions, the subspace specified by the conditions in (15) appears to be finite. This occurs because there exists a minimum positive value of the lightlike momentum  $p_- = \frac{\pi}{2L}$  and because the creation operators correspond only to positive values of  $p_-$ . An arbitrary state satisfying the conditions in (15) has the form

$$|\Psi\rangle = d_{N-1}^{+l_{2N}} \dots d_0^{+l_{N+1}} b_1^{+l_N} \dots b_N^{+l_1} |0\rangle, \quad l_i = 0, 1; \\ \sum_{i=1}^{2N} \text{sign} \left( N - i + \frac{1}{2} \right) l_i = 0, \quad \sum_{i=1}^{2N} \left| N - i + \frac{1}{2} \right| l_i = N, \quad (18)$$

where  $\text{sgn}$  is the sign function. The values  $l_i$  takes here only the values of 0 or 1 by virtue of the anticommutation relations (7).

The finiteness of the subspace that is specified by formulas (18) and where it is necessary to solve Eq. (14) reduces the problem to finding the eigenvalues of an  $N_{\text{mat}} \times N_{\text{mat}}$  finite matrix whose elements are specified by the matrix elements of the operator  $\frac{2\pi}{L} NH$  between the states in (18). A precise solution to this problem can be found numerically. The resulting eigenvalues will determine the squares  $M_i^2$  of bound-state masses. It should be noted that the dimension of the matrix,  $N_{\text{mat}}$ , grows fast as the parameter  $N$  increases – this is reflected in Table 1. In this

$N$	9	10	12	14	16	18	20	22	24	26	28	29	30
$N_{\text{mat}}$	31	43	78	136	232	386	628	1003	1576	2437	3719	4566	5605

Table 1. Relation between the parameter  $N$  and the dimensionality  $N_{\text{mat}}$  of the space of states.

study, the maximum achieved values of  $N$  are  $N = 30$  for the cases of  $\hat{\theta} = \theta = 0$  and  $\hat{\theta} = \theta = \pi$  and  $N = 28$  for the remaining cases.

As was mentioned above, the limit  $N \rightarrow \infty$  corresponds to the removal of the regularization. For this reason, it is not sufficient to calculate the mass spectrum  $M_i^2$  at the maximum accessible value of  $N$  – it is necessary to analyze the behavior of the spectrum as a function of  $N$  and to find the way to extrapolate the calculated values to the region of  $N \rightarrow \infty$ . We propose the following method of extrapolation. We introduce the quantity  $u = 1/N$  and consider the function  $M_i^2(u)$ . It is necessary to extrapolate the values of this function to zero. Our calculations reveal that the bound-state masses are sensitive to the parity of  $N$  – that is, there can occur a sharp change in  $M_i^2$  in response to the reversal of the parity of  $N$ . Therefore, it is reasonable to extrapolate the function  $M_i^2(u)$  to zero by two methods, individually in even and in odd values of  $N$ .

In order to extrapolate the function  $M_i^2(u)$  to zero, we approximate the dimensionless ratio  $M_i^2(u)/e^2$  by polynomials of various degrees by the least squares method. We denote by  $P_i(n)$  the value of a polynomial of degree  $n$  at zero. It is obvious that the maximum degree  $n$  that can be used is less by unity than the number of points at which the approximated function is known. In the present study, this degree is equal to 10 for the cases of  $\hat{\theta} = \theta = 0$  and  $\hat{\theta} = \theta = \pi$  and to 9 in the remaining cases (as the minimum value of  $N$ , we adopt  $N = 9$  in our calculations).

At different values of the ratio  $M/e$  and the parameter  $\hat{\theta}$ , there arise different types of behavior of  $P_i(n)$  as a function of  $n$ . In some cases, the function  $P_i(n)$  tends to a saturation and changes slowly with increasing  $n$  (see Fig. 1a). In these cases, the value at which the saturation occurs will be considered as the result of extrapolating the function  $M_i^2(u)/e^2$  to zero.

Sometimes, there arise oscillations against the background of a saturation (see Fig. 1b). This occurs if the error with which one calculates  $M_i^2(u)$  becomes sizable. In this case, a function that involves a noticeable random noise is approximated by a polynomial of high degree. This usually takes place at large values of the ratio  $M/e$ , in which case the coefficients of various terms of the Hamiltonian (5) differ from one another considerably. Conceptually, this situation does not differ from the preceding one. The value obtained by averaging the oscillations in the

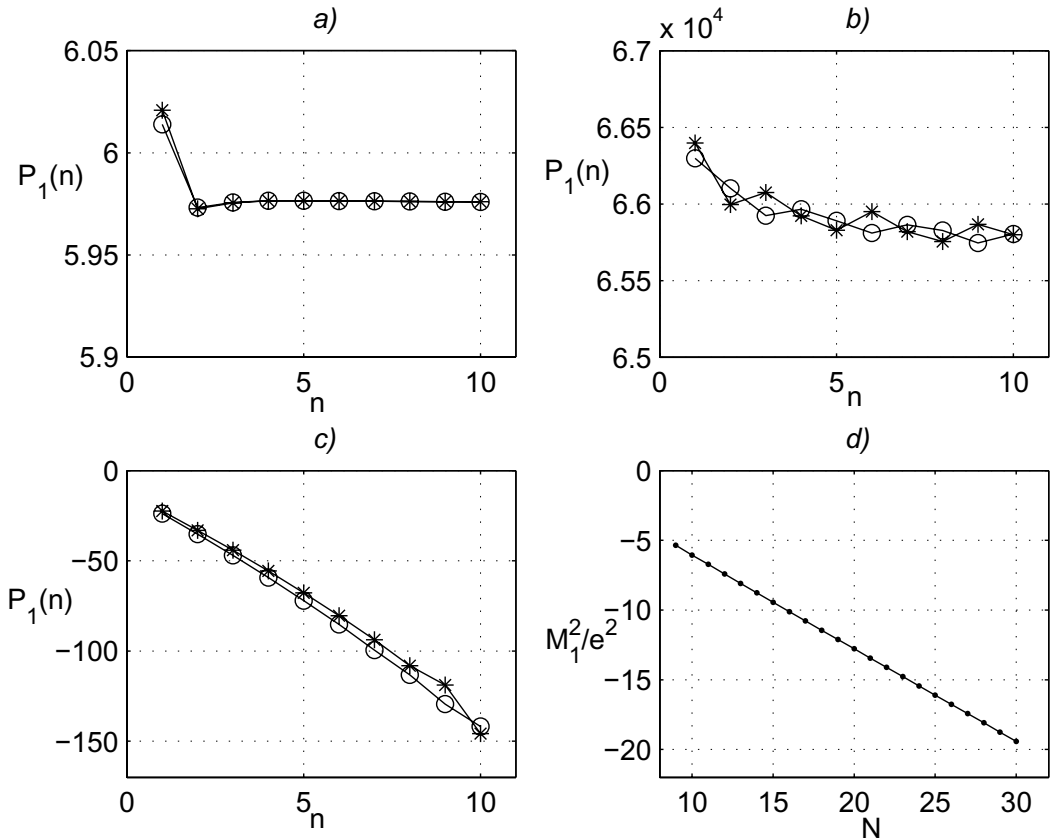


Fig. 1. Examples of the dependence of the extrapolated value of  $P_1(n)$  on the degree  $n$  of the approximating polynomial (a-c) and example of the dependence of the mass of the lowest bound state on  $N$  (d) for the following parameter values: (a)  $\hat{\theta} = \theta = 0$  and  $M/e = 1$ , (b)  $\hat{\theta} = \theta = 0$  and  $M/e = 2^7$ , and (c,d)  $\hat{\theta} = \theta = \pi$  and  $M/e = 0.5$ . The symbols  $\circ$  and  $*$  represent the results of the extrapolation in, respectively, even and odd values of  $N$ .

region of saturation will then be treated as the result of the extrapolation of the function  $M_i^2(u)/e^2$  to zero. It is obvious that the value found in this way will have an error larger than that in the preceding situation.

In the remaining cases, there arises the situation where the saturation cannot be seen – the function  $P_i(n)$  strongly changes with increasing  $n$  (see Fig. 1c). In order to discriminate between this case and the two preceding versions of behavior of the function  $P_i(n)$ , we introduce the measure of its relative variation in response to a considerable variation in the degree  $n$  of the polynomial (in the region of accessible values), for example, in the form

$$\xi = \sqrt{\frac{(P_i(4) - P_i(9))^2}{(P_i(4)^2 + P_i(9)^2)/2}}. \quad (19)$$

This quantity characterizes the error with which the calculated values of the mass spectrum  $M_i^2$  describe its limiting value. We will assume that, if  $\xi < 0.1$ , the saturation takes place for

the function  $P_i(n)$ , so that its value obtained at accessible  $n$  describes well the limiting value of the bound-state mass. But if  $\xi > 0.1$ , the calculated values of  $P_i(n)$  do not characterize the behavior of  $M_i^2$  in the limit  $N \rightarrow \infty$ . Moreover, the most frequently occurring form of the dependence  $P_i(n)$  suggests its linearly decreasing character (Fig. 1c). The same applies to the original dependence of the quantity  $M_i^2$  on the parameter  $N$  (see Fig. 1d). This gives sufficient grounds to assume that, at these values of the ratio  $M/e$  and the parameter  $\hat{\theta}$ , the quantity  $M_i^2$  tends to  $-\infty$  in the limit  $N \rightarrow \infty$ . The possible reasons behind this effect are discussed in the next section.

It should be noted that the choice of the value of 0.1 as a boundary one for the error in  $\xi$  and the specific choice of formula (19) are arbitrary to a considerable extent, but, unfortunately, our calculations could not provide a more rigorous way to discriminate between the situations where the limit of the quantity  $M_i^2$  for  $N \rightarrow \infty$  exists and where  $M_i^2$  tends to  $-\infty$  in the same limit.

#### 4. Results of the calculations

##### 4.1. Case of $\hat{\theta} = \theta = 0$ .

In the case of  $\theta = 0$ , the mass spectrum of the massive Schwinger model in Lorentz coordinates has received quite an adequate study (see [13, 16] and references therein). Usually, one studies the masses  $M_1$  and  $M_2$  of the first two bound states, which are referred to as a vector and a scalar state, respectively. The most accurate results were obtained in [14] with the aid of lattice calculations. Table 2 presents the values of  $(M_1 - 2M)/e$  and  $(M_2 - 2M)/e$  (it is precisely these quantities that were calculated in [14]) that were found by the method proposed here (with the aid of an extrapolation to the limit  $N \rightarrow \infty$ ) and the values of these quantities from [14]. In the case of  $\theta = 0$ , the error  $\xi$  does not exceed the threshold of 0.1 at any values of the ratio  $M/e$  that were considered here (more specifically,  $\xi < 0.01$  for  $M_1$  and  $\xi < 0.03$  for  $M_2$ ) – that is, the above procedure of extrapolation to the limit  $N \rightarrow \infty$  provides quite reliable results.

Figure 2a gives the extrapolated values of  $(M_1 - 2M)/e$  along with the results obtained in [14]. The displayed errors were found from the corresponding values of the relative error  $\xi$ . In this figure, we also present the results corresponding to the maximum accessible value of  $N = 30$  – that is, the results obtained without extrapolation. It can be seen that these results are accurate only at small values of  $M/e$ ; at the same time, the extrapolated values give a very good result up to  $M/e = 8$ . For  $M/e > 8$ , the extrapolated values reproduce a correct result within the error, which begins growing fast in this region. This is because the ratio  $M/e$  becomes large in this region, with the result that the absolute error of the difference  $(M_1 - 2M)/e$  appears to be large even at a small relative error in the calculated quantity  $M_1^2/e^2$ . In order to depict the calculated results over the entire wide region of  $M/e$ , it is convenient to plot the normalized values

$$M_i^{\text{norm}} = \frac{M_i}{\sqrt{m^2 + (2M)^2}}, \quad (20)$$

as was proposed in [16]. These normalized values possess the property that  $M_1^{\text{norm}} \rightarrow 1$  both in the limit  $M \rightarrow 0$  and in the limit  $e \rightarrow 0$ . In Fig. 2b, we show the curves for  $M_1^{\text{norm}}$  that

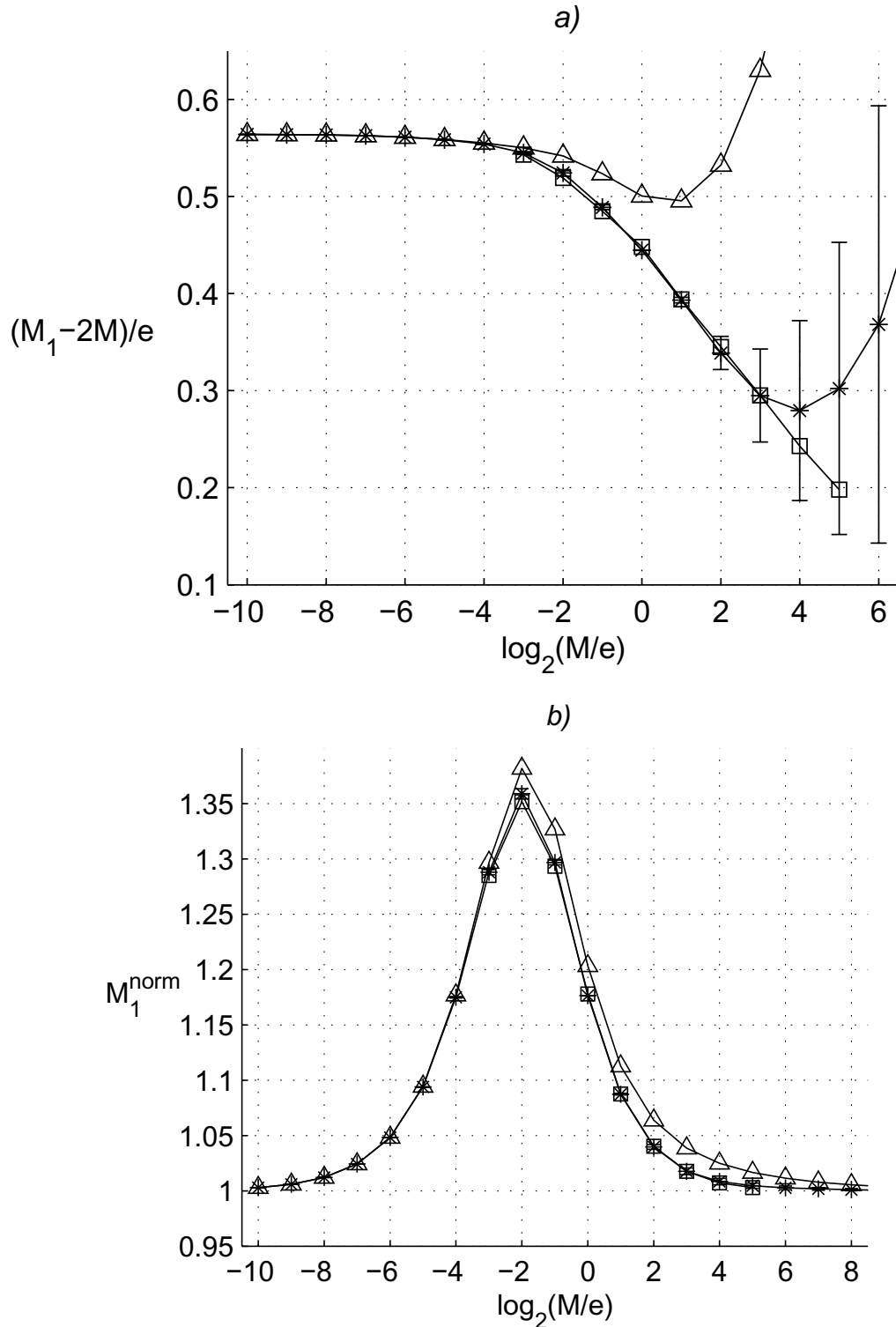


Fig. 2. Calculated mass  $M_1$  of the vector bound state at  $\hat{\theta} = \theta = 0$ ; \* – results obtained by extrapolation to the limit  $N \rightarrow \infty$ ,  $\triangle$  – results of the calculation at  $N = 30$ ,  $\square$  – results borrowed from [14].

$M/e$	$(M_1 - 2M)/e$		$(M_2 - 2M)/e$	
	our study	[14]	our study	[14]
$2^{-10}$	0.564		1.13	
$2^{-9}$	0.564		1.13	
$2^{-8}$	0.563		1.13	
$2^{-7}$	0.563		1.14	
$2^{-6}$	0.561		1.15	
$2^{-5}$	0.559		1.17	
$2^{-4}$	0.554		1.20	
$2^{-3}$	0.545	0.543	1.23	1.22
$2^{-2}$	0.524	0.519	1.24	1.24
$2^{-1}$	0.489	0.485	1.20	1.20
$2^0$	0.445	0.448	1.12	1.12
$2^1$	0.393	0.394	0.99	1.00
$2^2$	0.339	0.345	0.84	0.85
$2^3$	0.295	0.295	0.75	0.68
$2^4$	0.279	0.243	0.74	0.56
$2^5$	0.302	0.198	0.84	0.45
$2^6$	0.368		1.08	
$2^7$	0.497		1.41	
$2^8$	0.619			

Table 2. Masses of the vector ( $M_1$ ) and scalar ( $M_2$ ) bound states according to the calculations performed in the present study and in [14] at  $\hat{\theta} = \theta = 0$  and various values of the ratio  $M/e$ .

correspond to those in Fig. 2a. One can see that the extrapolated values agree with the results from [14] to a high precision over the entire range of  $M/e$ .

In Fig. 3, the extrapolated values of  $M_1^{\text{norm}}$  that were calculated on the basis of the corrected Hamiltonian (5) are contrasted against the analogous values corresponding to the Hamiltonian obtained upon the naive light-front canonical quantization of the fermion theory specified by Eq. (2) that is, to expression (5) where one discards the second term [see the comment before formula (13)] and those corresponding to the Hamiltonian obtained upon the naive light-front canonical quantization of the boson theory specified by Eq. (4) that is, to expression (5) where one discards the third term and replaces  $\hat{\theta}$  by  $\theta$ , as was shown in [21, 22]. One can see from this figure that the naive light-front canonical quantization of the fermion formulation of the theory gives good results at large values of the ratio  $M/e$  – that is, in the region of weak coupling–while the analogous quantization of the boson formulation of the theories gives good results at small values of this ratio – that is, in the region of strong coupling. In order to obtain a light-front Hamiltonian that would provide good results at any values of the ratio  $M/e$ , it is necessary to implement the procedure of correcting the naive Hamiltonian, as was done in [21, 22].

In Fig. 4, we give the curves that represent the mass  $M_2$  of the scalar bound state and which are analogous to those in Fig. 2a for the mass  $M_1$  of the vector bound state. The behavior of the curves is identical to that in the case of the vector state: the values corresponding to

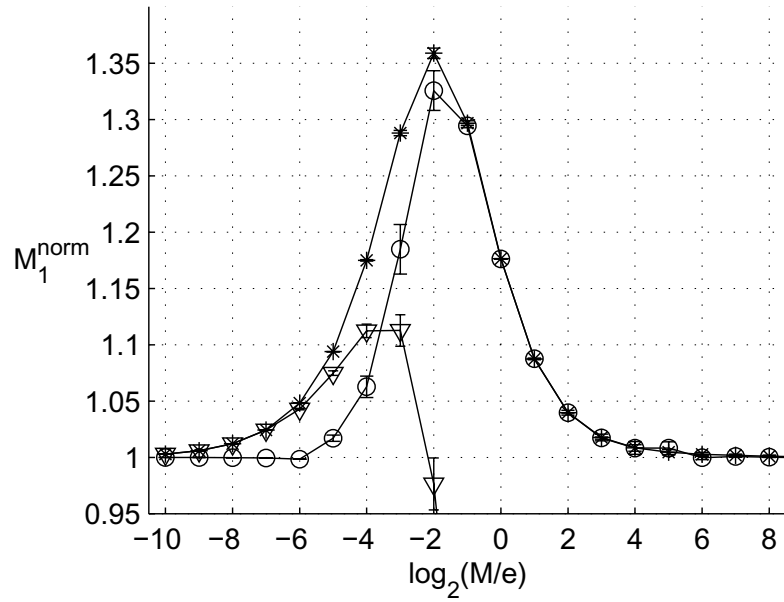


Fig. 3. Calculated mass  $M_1$  of the vector bound state at  $\hat{\theta} = \theta = 0$ ; \* – results obtained with the aid of the corrected light-front Hamiltonian,  $\circ$  and  $\nabla$  – result obtained by means of the naive light-front quantization of, respectively, the fermion and the boson formulation of the theory.

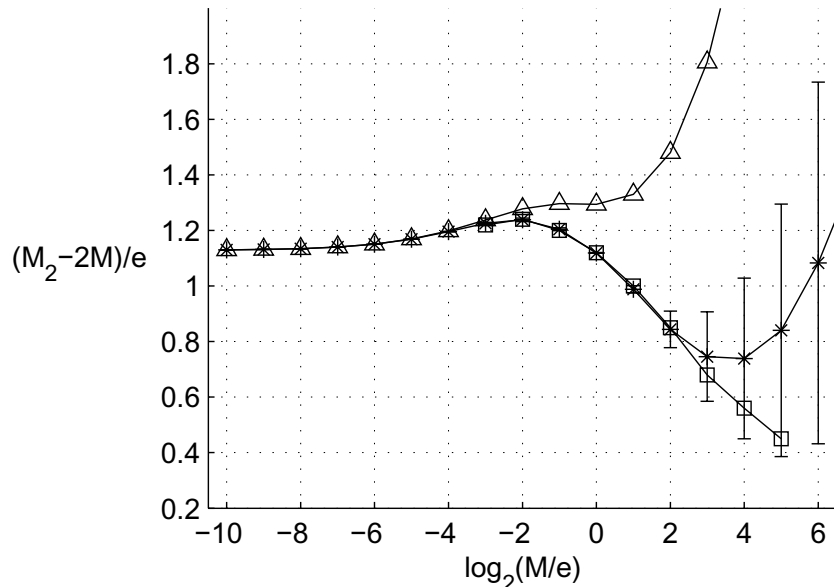


Fig. 4. Calculated mass  $M_2$  of the scalar bound state at  $\hat{\theta} = \theta = 0$ ; \* – results obtained by means of an extrapolation to the limit  $N \rightarrow \infty$ ,  $\triangle$  – results corresponding to  $N = 30$ ,  $\square$  – results borrowed from [14].

$N = 30$  give good results only at small values of  $M/e$ , while the extrapolated values give very good results up to  $M/e = 4$  and reproduce the correct result within the error for  $M/e > 4$ .

#### 4.2. Case of $\hat{\theta} = \theta = \pi$ .

The value of  $\theta = \pi$  is of particular importance in the theory. It was predicted in [18] that, at  $\theta = \pi$ , a phase transition occurs in the theory at some value of the ratio  $M/e$ , so-called semi asymptotic fermions appearing in the region below the phase transition. In the region above the phase transition, as well as in the case where  $\theta \neq \pi$ , confinement takes place. More recent calculations, performed for  $\theta = \pi$  revealed (see, for example, [13]) that the phase transition occurs at  $M/e = 0.33$ .

By means of lattice calculations, the mass of the lowest state in the electron-positron (two-particle) sector as a function of  $M/e$  at  $\theta = \pi$  was studied in [13]. Within our approach, this mass corresponds to the quantity  $M_1$ .

In Fig. 5, the extrapolated values of  $M_1/e$  are given along with the results reported in [13]. One can see that, at small values of the ratio  $M/e$ , these results agree well, but that

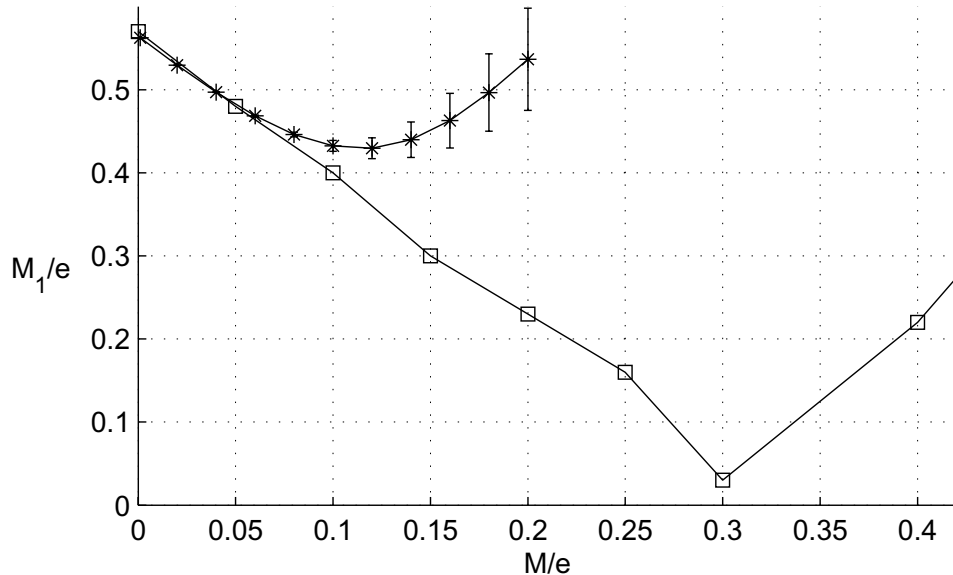


Fig. 5. Calculated mass  $M_1$  of the lowest bound state at  $\hat{\theta} = \theta = \pi$ ; \* – results obtained by means of an extrapolation to the limit  $N \rightarrow \infty$ ,  $\square$  – results borrowed from [13].

this agreement deteriorates as the ratio  $M/e$  grows. For  $M/e > 0.14$ , the extrapolation error  $\xi$  [see formula (19)] exceeds 0.1; therefore, the corresponding points on the graph are not quite reliable. For  $M/e > 0.21$ , there sharply appear very large oscillations in the behavior of the corresponding functions  $P_1(n)$  describing the dependence of the extrapolated values on the degree of the approximating polynomial [see Section 3, the text before Eq. (19)]. At  $M/e = 0.4$ , the oscillations virtually disappear, whereupon the dependence begins displaying a linearly decreasing character. By way of example, this dependence at  $M/e = 0.5$  is depicted in Fig. 1c, while the corresponding dependence of the quantity  $M_1^2/e^2$  on  $N$  (it is also manifestly linear) is shown in Fig. 1d. For  $M/e > 0.2$ , the extrapolation error  $\xi$  exceeds 0.5.

The linear decrease in  $M_1^2/e^2$  with increasing  $N$  gives sufficient grounds to assume that this quantity tends to  $-\infty$  in the limit  $N \rightarrow \infty$ . This means that, at the above values of the ratio  $M/e$  and the parameter  $\hat{\theta}$ , the spectrum of the Hamiltonian in (5) upon the removal of the regularization appears to be not bounded from below, so that the theory specified by this Hamiltonian is incorrect. This situation is possible in the case where there arise effects that are purely nonperturbative from the point of view of perturbation theory in the fermion mass  $M$  since the Hamiltonian in (5) was constructed by analyzing such a perturbation theory (in all orders). Obviously, the presence of the aforementioned phase transition is a nonperturbative effect in this case. One can conclude that above the phase-transition point ( $M/e = 0.33$ ), the theory generated by the light-front Hamiltonian (5) becomes incorrect; at the same time, the original theory in Lorentz coordinates, which is specified by Eq. (2), remains correct, this being corroborated by the results reported in [13] for the region above the phase-transition point.

The appearance of the aforementioned strong oscillations of the functions  $P_1(n)$  in the range  $0.2 < M/e < 0.4$  is likely to be associated with the proximity of the phase-transition point, where the regularization, which is parametrized by the number  $N$ , can distort the theory more strongly than as usual. It can also be conjectured that a sizable deviation of the extrapolated values of  $M_1/e$  from the results of paper [13] in the upper part of the region  $M/e < 0.2$  is due to the same factor.

#### 4.3. Case of Intermediate Values of $\hat{\theta}$ .

As was indicated above, the quantity  $\hat{\theta}$  is a function of the ratio  $M/e$  and the parameter  $\theta$ , this function being specified in the form of an infinite series in  $M$ . Therefore, the relation between  $\hat{\theta}$  and  $\theta$  is a priori unknown [this is not so only in the particular cases of  $\theta = 0, \pi$  (see above)]. In principle, this relation can be sought by comparing the mass spectrum calculated on the basis of the light-front Hamiltonian (5), which depends on  $\hat{\theta}$ , and the spectrum calculated in Lorentz coordinates at a specific vacuum angle  $\theta$ .

It can be shown that the mass spectrum of the theory is invariant under the reversal of the sign of the quantities  $\hat{\theta}$  and  $\theta$  (it should be recalled that  $\hat{\theta}$  is an odd function  $\hat{\theta}$ ). This can be seen most straightforwardly in the boson form of the theory (4), where the reversal of the sign of  $\theta$  is equivalent to the replacement ( $\varphi$  by  $-\varphi$ , which does not change the mass spectrum). However, this invariance can be directly seen from the Hamiltonian in (5). One can show that it does not change if we reverse the sign of  $\hat{\theta}$  and simultaneously interchange the operators  $d_n$  and  $b_{n+1}$  (in this case,  $\omega$  is replaced by  $-\omega$ ). This is a unitary transformation and does not change the mass spectrum. Thus, it is sufficient to perform calculations of the mass spectrum for the case where the parameter  $\hat{\theta}$  lies between 0 and  $\pi$ .

For the lowest bound state, the mass  $M_1$  calculated in this way and normalized according to (20) is displayed in Fig. 6. Each curve corresponds to a fixed value of the quantity  $\hat{\theta}$  from the set  $0, 0.05\pi, 0.1\pi, \dots, \pi$ . Each successive curve (for increasing  $\hat{\theta}$ ) lies below the preceding one. In the cases of  $\hat{\theta}/\pi = 0$  and  $\hat{\theta}/\pi = 0.05$  (the first and the second curve from above), the extrapolation error  $\xi$  [see (19)] does not exceed 0.1 at any values of  $M/e$ .

In the case of  $\hat{\theta}/\pi = 0.1$ ,  $\xi > 0.1$  at  $M/e$  values in the range between 2 and  $2^4$ ; therefore, it is meaningless to plot the corresponding points on the graph, so that the curves decompose into two parts. In this region, the corresponding functions  $P_1(n)$  (used in the extrapolation) display a manifest linearly decreasing character. This situation is similar to that considered in Subsection 4.2 for the case of  $\theta = \pi$ . It can be concluded that, in the region being considered, the theory specified by the Hamiltonian in (5) becomes incorrect upon the removal of the

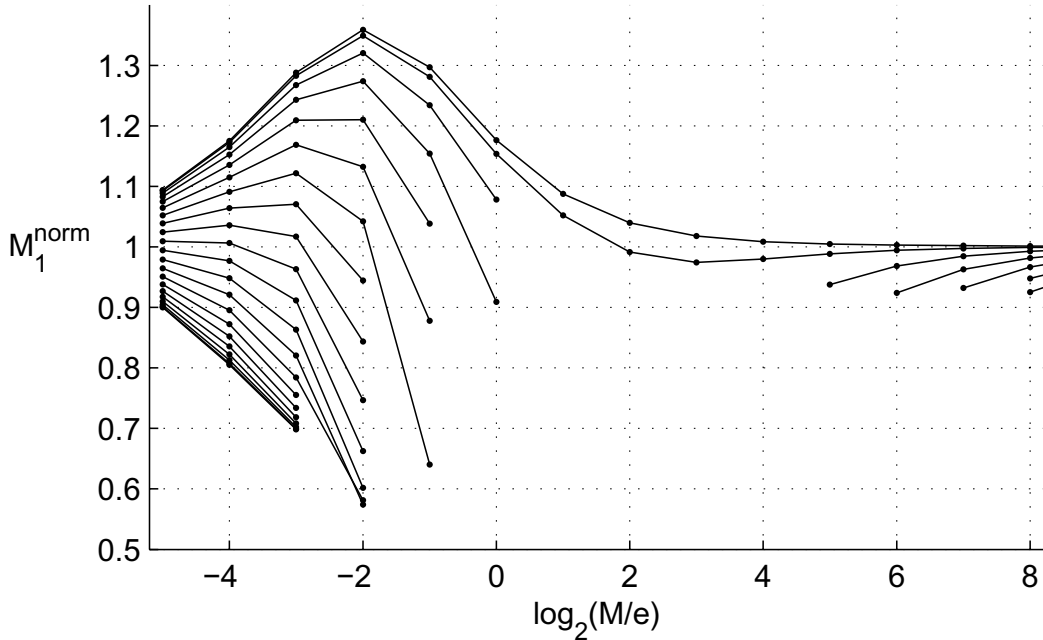


Fig. 6. Calculated mass  $M_1$  of the lowest bound state as a function of  $M/e$  at various values of the parameter  $\hat{\theta}$ :  $0, 0.05\pi, 0.1\pi, \dots, \pi$ . As the parameter  $\hat{\theta}$  is increased, the curve is shifted downward.

regularization, and it can be assumed that, in the vicinity of the point  $M/e = 2$ , there exists some nonperturbative effect as in the case of  $\theta = \pi$  (see Subsection 4.2).

In principle, it can be assumed that a nonperturbative effect exists in the vicinity of the point  $M/e = 2^4$  as well, above which the error  $\xi$  again falls below 0.1. However, it seems more probable that, in the region of large values of  $M/e$ , the Hamiltonian remains unbounded from below upon the removal of the regularization, but the decrease in the mass of the lowest state with increasing regularization parameter  $N$  is so slow that  $\xi$  appears to be less than 0.1. This is favored by the dependence  $P_1(n)$  which, at large values of  $M/e$ , has the form of a linear function with a moderate slope that yields  $\xi < 0.1$ . As was discussed at the end of Section 3, there is unfortunately no method for discriminating between the situations where, in the limit  $N \rightarrow \infty$ , there exists the limit of the mass of the lowest state and where this mass tends to  $-\infty$ .

In the cases of  $\hat{\theta}/\pi = 0.15, \dots, 0.3$ , the situation is perfectly analogous to that in the case of  $\hat{\theta}/\pi = 0.1$  (only the width of the region where  $\xi > 0.1$  changes), which was considered immediately above, while, at  $\hat{\theta}/\pi = 0.35, \dots, 1$  the difference consists in that the region where  $\xi < 0.1$  at large values of  $M/e$  is not reached at the  $M/e$  values considered here.

In Fig. 7, the points where the extrapolation error  $\xi$  is less than 0.1 are shown in the plane spanned by the parameters  $M/e$  and  $\hat{\theta}$ . It is natural to assume that, in the region where there are no points in the figure, the light-front Hamiltonian (5) is unbounded from below upon the removal of the regularization,  $N \rightarrow \infty$ .

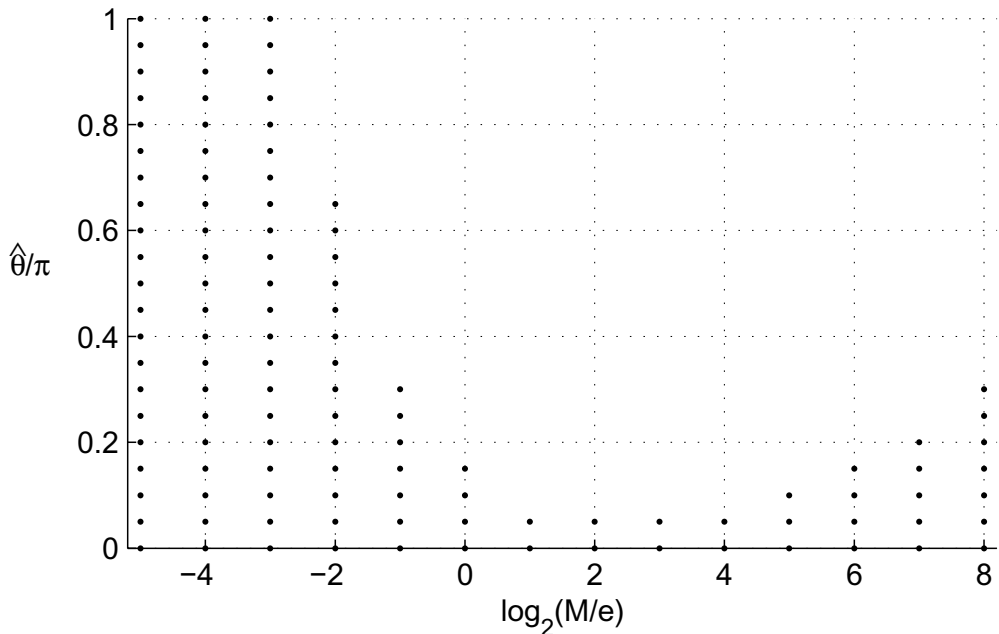


Fig. 7. Set of pairs of  $M/e$  and  $\hat{\theta}$  values at which the extrapolation error  $\xi$  is less than 0.1.

## 5. Conclusion

A numerical nonperturbative calculation of the mass spectrum of QED-2 (massive Schwinger model) has been performed by the method of discrete light-cone quantization. In doing this, use has been made of the corrected light-front Hamiltonian (that is, that which generates a theory that is equivalent in all orders of perturbation theory in the fermion mass  $M$  to the Lorentz-covariant formulation of QED-2) constructed in [21, 22]. The results obtained in this way have been compared with the results of the numerical calculations on a lattice in Lorentz coordinates from [14, 13].

Since actual calculations are performed at a finite value of the infrared-regularization parameter  $N$ , a method has been proposed for extrapolating the results of these calculations to the region of  $N$  tending to infinity, this corresponding to the removal of this regularization. As the result of this extrapolation, it becomes clear that, at some values of the parameters of the theory, its mass spectrum is not bounded from below in the limit where the regularization is removed. This occurs only at rather large values of the fermion mass  $M$ ; therefore, it is natural to assume that, in this region, the Hamiltonian used becomes incorrect, since it was constructed via an analysis of perturbation theory in  $M$ .

The calculations have been performed over a wide range of the fermion mass  $M$  for all values of the Hamiltonian parameter  $\hat{\theta}$ , which is a function of the ratio  $M/e$  and the vacuum angle  $\theta$ . This function, which is a priori unknown possesses the property that it vanishes at  $\theta = 0$  and is equal to  $\pi$  at  $\theta = \pi$ .

At zero value of the vacuum angle  $\theta$ , the resulting spectrum is bounded from below at any value of  $M$ , and the values obtained in this case for the two lowest bound states reproduce well

the results reported in [14].

At the vacuum-angle value of  $\theta = \pi$ , which is special for the theory being considered, the masses found here for the lowest bound state agree well with the results of paper [13] for rather low values of  $M$ ; as the mass  $M$  increases, there first arises a discrepancy, whereupon the spectrum of the theory become unbounded from below. Since the  $M$  value at which this takes place is approximately equal to that at which there occurs a phase transition in the theory (see, for example, [13])), it would be reasonable to assume that, at  $M$  values above the phase-transition point, the light-front Hamiltonian used here, which was constructed on the basis of an analysis of perturbation theory in  $M$ , becomes incorrect.

Our calculations have revealed that, in the case of QED-2, the procedure employed in [21, 22] to construct the corrected light-front Hamiltonian leads to a Hamiltonian that yields good results in nonperturbative calculations. By exploring the question of how the spectrum of the Hamiltonian changes in response to changes in the parameters of the theory from the perturbative region of their values, one can determine the boundaries of the applicability region of this Hamiltonian – that is, to find the region where it is necessary to take additionally into account nonperturbative (for example, vacuum) effects. This may be of use in studying more realistic gauge field theories.

The LF Hamiltonian (5), used in the present paper for the calculation of bound state mass, includes the operator  $\omega$ , which has no simple expression in terms of field operators. It is defined only by its properties (10)-(12). Due to this fact the expression for the Hamiltonian depends essentially on the form of the regularization, i.e.  $|x^-| \leq L$  and antiperiodic boundary conditions in  $x^-$  for the field  $\psi$ . Now we have found a possibility to rewrite the expression (5) in such a way that it contains only fermion field operators, and describes in the limit of removing the regularizations the same theory as the Hamiltonian (5). This new expression has at  $\hat{\theta} = \theta = 0$  the following form:

$$H = \int_{-L}^L dx^- \left( \frac{e^2}{2} \left( \partial_-^{-1} [\psi^+ \psi] \right)^2 + \frac{eMe^C}{4\pi^{3/2}} \left( d_0^+ d_0 + b_1^+ b_1 \right) - \frac{iM^2}{2} \psi^+ \partial_-^{-1} \psi \right). \quad (21)$$

Preliminary calculations of the mass spectrum, produced by this Hamiltonian, show that in the limit of removing the regularization,  $L \rightarrow \infty$ , results indeed coincide, with a good accuracy, with those for the bound state mass spectrum found here for the Hamiltonian (5). Work on studing of the Hamiltonian (21) spectrum and also on the constructing the analogous expression for the Hamiltonian at  $\hat{\theta} \neq 0$  will be continued in future.

**Acknowledgments.** The work was supported by the administration of St. Petersburg and the Ministry of Education of the Russian Federation, grant no. PD03-1.2-35 (S.A.P.), and by the Russian Foundation for Basic Research, grant no. 05-02-17477 (S.A.P. and E.V.P.).

## Appendix

Let us find out how the parameter  $\hat{\theta}$ , which is a function of the ratio  $M/e$  and the vacuum angle  $\theta$ , appears in the light-front Hamiltonian (5). It was shown in [21, 22] that the coefficient of the operator  $e^{i\omega} d_0^+$  in the integrand on the right-hand side of (5) is the limit of the quantity  $-B^*$  (\* denotes the operation of complex conjugation) in the limit  $w \rightarrow \infty$  (which corresponds

to removing the intermediate ultraviolet regularization), where  $B$  is given by

$$B = -\frac{1}{2w} + \sqrt{\frac{1}{4w^2} + \frac{A'}{w} - A''^2 + iA''}. \quad (\text{A.1})$$

Here,  $A'$  and  $A''$  are, respectively, the real and the imaginary part of the sum (calculated in Lorentz coordinates and in all orders in  $\gamma$ , including the first order)

$$A = \frac{\gamma}{2}e^{i\theta} + \sum_{k=2}^{\infty} A_k \gamma^k \quad (\text{A.2})$$

of all connected diagrams of the boson theory specified by the Lagrangian (4) which have a property that all their external lines connect with the one vertex  $\frac{\gamma}{2}e^{i\theta}$  [the propagators of the external lines and a common factor that depends on their number are not included in the definition of  $A$ , as can be seen from the first term in (A.2)]. In [21], it was established that, in the limit  $w \rightarrow \infty$ , the quantities  $A_k$  for  $k \neq 2$  are finite, while  $A_2$  behaves as

$$A_2 = \frac{\gamma^2}{4}w + \text{const.} \quad (\text{A.3})$$

Expression (A.1) was deduced from an analysis of perturbation theory in  $\gamma$  (in all orders). As a matter of fact, the series that can be obtained by substituting expansion (A.2) into (A.1) provides the definition of the quantity  $B$ . One can see that the first term of this series is linear in  $\gamma$  and, at large  $w$ , its radius of convergence varies in proportion to  $1/w$ . As was mentioned above, it is necessary to find the limit of the quantity  $B$  for  $w \rightarrow \infty$ . Since the aforementioned radius of convergence tends to zero in this limit, it is obvious that, before going to the limit, the quantity  $B$  must be continued analytically in  $\gamma$  to the region of positive  $\gamma$  values, which lie beyond the disk determined by this radius of convergence. For this, we determine the behavior of radicand on the right-hand side of (A.1) at large  $w$  and  $\gamma$  of about  $1/w$ . Taking into account (A.3), we obtain

$$\sqrt{\frac{1}{4w^2} + \frac{A'}{w} - A''^2} = \frac{1}{2w} \sqrt{(1 + w\gamma \cos \theta)^2 + O\left(\frac{1}{w}\right)}. \quad (\text{A.4})$$

From here, we find that there exist two branch points, whose positions are given by the formula

$$\gamma_{1,2} = -\frac{1}{w \cos \theta} + O\left(\frac{1}{w^{3/2}}\right). \quad (\text{A.5})$$

It can be concluded from formulas (A.4) and (A.5) that, in the limit  $w \rightarrow \infty$ , the sought analytic continuation of the quantity  $B$  has the form

$$B = \text{sign}(\cos \theta) \sqrt{\frac{\gamma^2}{4} - A''^2 + iA''} = \frac{\gamma}{2} e^{i\hat{\theta}}. \quad (\text{A.6})$$

The form of this expression corresponds to the form of the coefficient of the operator  $e^{i\omega} d_0^+$  in Hamiltonian (5). Expression (A.6) differs by the presence of the sign function  $\text{sign}(\cos \theta)$  from the corresponding expression presented in [21, 22], where the features of the analytic

continuation of  $B$  were not taken into account. In the first order in  $\gamma$  (and, hence, in  $M$ ), we find from (A.6), with the aid of expansion (A.2), that  $\hat{\theta} = \theta$ .

Upon the Euclidean rotation in the diagrams determining the quantity  $A$ , it becomes clear  $A$  is a real-valued function of  $m$ ,  $\gamma$ ,  $e^{i\theta}$  and  $e^{-i\theta}$ . It follows from here that the reversal of the sign of the parameter  $\theta$  is equivalent to the complex conjugation of the quantity  $A$ , this quantity being real-valued at  $\theta = \pi$ . By using these facts and formula (A.6), one can easily see that  $\hat{\theta}$  is an odd function of  $\theta$  and, in addition, that  $\hat{\theta} = \pi$  at  $\theta = \pi$ .

## References

- [1] P. A. M. Dirac, Rev. Mod. Phys. **21**, 392 (1949).
- [2] S. J. Brodsky, H.-C. Pauli, S. S. Pinsky, Phys. Rep. **301**, 299 (1998), hep-ph/9705477.
- [3] V. A. Franke, Yu. V. Novozhilov, S. A. Paston, E. V. Prokhvatilov, in book: *Quantum Theory in Honour of Vladimir A. Fock, Part 1* (Unesco, St. Petersburg University, Euro-Asian Physical Society, 1998), p. 38, hep-th/9901029.
- [4] A. M. Annenkova, E. V. Prokhvatilov, V. A. Franke, Vestn. LGU, No. 4, 80 (1985).
- [5] V. A. Franke, Yu. V. Novozhilov, E. V. Prokhvatilov, Lett. Math. Phys. **5**, 239 (1981).
- [6] V. A. Franke, Yu. V. Novozhilov, E. V. Prokhvatilov, Lett. Math. Phys. **5**, 437 (1981).
- [7] A. M. Annenkova, E. V. Prokhvatilov, V. A. Franke, Phys. At. Nucl. **56**, 813 (1993).
- [8] E. V. Prokhvatilov, V. A. Franke, Sov. J. Nucl. Phys. **49**, 688 (1989).
- [9] E. V. Prokhvatilov, H. W. L. Naus, H.-J. Pirner, Phys. Rev. D **51**, 2933 (1995), hep-th/9406275.
- [10] M. Burkardt, A. Langnau, Phys. Rev. D **44**, 1187, 3857 (1991).
- [11] S. A. Paston, V. A. Franke, Theoretical and Mathematical Physics **112**, 1117 (1997), hep-th/9901110.
- [12] S. A. Paston, V. A. Franke, E. V. Prokhvatilov, Theoretical and Mathematical Physics **120**, 1164 (1999), hep-th/0002062.
- [13] T. Byrnes, P. Sriganesh, R.J. Bursill, C.J. Hamer, Phys. Rev. D **66**, 013002 (2002), hep-lat/0202014.
- [14] P. Sriganesh, C.J. Hamer, R.J. Bursill, Phys. Rev. D **62**, 034508 (2000), hep-lat/9911021.
- [15] C. Adam, Ann. Phys. **259**, 1 (1997), hep-th/9704064.
- [16] C. Adam, Phys. Lett. B **555**, 132 (2003), hep-th/0212171.
- [17] G. McCartor, Phys. Rev. D **60**, 105004 (1999).

- [18] S. Coleman, Ann. Phys. **101**, 239 (1976).
- [19] E. V. Prokhvatilov, Teor. Mat. Fiz. **88**, 685 (1991).
- [20] S. A. Paston, E. V. Prokhvatilov, V. A. Franke, Theoretical and mathematical physics **136**, 951 (2003), hep-th/0310053.
- [21] S. A. Paston, E. V. Prokhvatilov, V. A. Franke, hep-th/0011224.
- [22] S. A. Paston, E. V. Prokhvatilov, V. A. Franke, Theoretical and mathematical physics **131**, 516 (2002), hep-th/0302016.
- [23] E. V. Prokhvatilov, V. A. Franke, Phys. At. Nucl. **59**, 2030 (1996).